



HAL
open science

Iron from continental weathering dictated soft-part preservation during the Early Ordovician

Farid Saleh, Victoire Lucas, Bernard Pittet, Bertrand Lefebvre, Stefan Lalonde,
Pierre Sansjofre

► **To cite this version:**

Farid Saleh, Victoire Lucas, Bernard Pittet, Bertrand Lefebvre, Stefan Lalonde, et al.. Iron from continental weathering dictated soft-part preservation during the Early Ordovician. *Terra Nova*, 2022, 34 (3), pp.163-168. <10.1111/ter.12572>. <hal-03852421>

HAL Id: hal-03852421

<https://hal.science/hal-03852421v1>

Submitted on 15 Nov 2022

HAL is a multi-disciplinary open access archive for the deposit and dissemination of scientific research documents, whether they are published or not. The documents may come from teaching and research institutions in France or abroad, or from public or private research centers.

L'archive ouverte pluridisciplinaire **HAL**, est destinée au dépôt et à la diffusion de documents scientifiques de niveau recherche, publiés ou non, émanant des établissements d'enseignement et de recherche français ou étrangers, des laboratoires publics ou privés.



HAL Authorization

1 Iron from continental weathering dictated soft-part preservation during the Early
2 Ordovician

3 **Farid Saleh^{1,2*}, Victoire Lucas³, Bernard Pittet³, Bertrand Lefebvre³, Stefan V.
4 Lalonde⁴, Pierre Sansjofre⁵**

5
6 ¹ Yunnan Key Laboratory for Palaeobiology, Institute of Palaeontology, Yunnan University,
7 Kunming, China

8 ² MEC International Joint Laboratory for Palaeobiology and Palaeoenvironment, Institute of
9 Palaeontology, Yunnan University, Kunming, China

10 ³ Université de Lyon, Université Claude Bernard Lyon 1, École Normale Supérieure de Lyon,
11 CNRS, UMR5276, LGL-TPE, Villeurbanne, France

12 ⁴ University of Brest, CNRS, IUEM Institut Universitaire Européen de la Mer, UMR 6538
13 Laboratoire Géosciences Océan, Place Nicolas Copernic, 29280 Plouzané, France

14 ⁵ MNHN, Sorbonne Université, CNRS UMR 7590, IRD, Institut de Minéralogie, Physique des
15 Matériaux et de Cosmochimie, Paris, France

16 Corresponding authors:

17 F. Saleh (farid.nassim.saleh@gmail.com)

18
19 **SHORT RUNNING TITLE:** Continental Fe in the Fezouata Shale

20 21 **DATA AVAILABILITY STATEMENT**

22 The data that supports the findings of this study are available in the supplementary material of
23 this article.

24 25 **ETHICAL AND CONFLICT OF INTEREST STATEMENTS**

26 We hereby confirm that all the data and interpretations are new and have not been published
27 elsewhere. All authors have been involved in this work, and approved the manuscript and
28 agreed to this submission. Authors declare having no conflict of interest, and that they
29 developed this study ethically, and according to the guidelines of Terra Nova.

30 31 **STATEMENT OF SIGNIFICANCE**

32 The Fezouata Shale (Morocco) is one of the rare sites preserving a diverse fossil assemblage
33 with soft parts in the Ordovician. Fe played a role in the preservation of these labile
34 anatomies. Here, it is shown that this Fe had a continental origin highlighting the importance
35 of continental Fe fluxes in the preservation of soft parts during the initial stages of the
36 Ordovician Radiation.

37 38 **ABSTRACT**

39 The Fezouata Shale in Morocco is the most diverse Lower Ordovician unit yielding soft-
40 tissue preservation. Iron played a crucial role in the preservation of soft parts in this formation
41 through the damage of bacterial membranes under oxic conditions and the pyritization of soft
42 parts under the activity of bacterial sulfate reduction. However, the origin of Fe in this
43 formation remains largely speculative. Herein, trace and rare earth elements were investigated
44 in drilled-core sediments from the Fezouata Shale. It is shown that a correlation exists
45 between Fe and Al suggesting that most Fe has a detrital source. Elemental concentrations in
46 the Fezouata Shale are most comparable to rivers and are the least similar to loess and
47 sediments deposited near active island arcs. In this sense, continental weathering and its
48 related Fe in river fluxes dictated occurrences of exceptional fossil preservation in the
49 Fezouata Shale.

51 INTRODUCTION

52 Exceptional fossil preservation, consisting of the preservation of soft anatomies in the rock
53 record, is crucial to reconstruct accurate pictures of ancient ecosystems (Butterfield, 1995;
54 Hou et al., 2004; Van Roy et al., 2010; Fu et al., 2020; Nanglu et al., 2020; Saleh et al.,
55 2020a, 2021a). The Fezouata Shale discovered in Morocco is an Early Ordovician deposit
56 bearing a large number of taxa that were previously unknown from this time interval (Van
57 Roy et al., 2010, 2015; Martin et al. 2016). Exceptionally preserved fossils in the Fezouata
58 Shale are discovered in levels that are relatively rich in iron (Saleh et al., 2019). It has been
59 experimentally shown that Fe among other cations and Fe-rich clay minerals slow down the
60 activity of decaying bacteria under oxic conditions through the destruction of bacterial
61 membranes (Imlay et al., 1988; Butterfield, 1990; Guida et al., 1991; Kapoor and Arora,
62 1998; Petrovich, 2001; Amonette et al., 2003; Wilson and Butterfield, 2014; McMahon et al.,
63 2016). In this sense, Fe availability in specific levels within the Fezouata Shale prevented the
64 complete loss of labile anatomies (Saleh et al., 2020b, c). Moreover, Fe plays a major role in
65 the fossilization of soft parts when bacterial-sulfate reduction (BSR) conditions are
66 established (Raiswell et al., 1993; Gabbott et al., 2004; Saleh et al., 2020b, c). Under BSR
67 conditions, Fe reacts with H₂S produced through the decay of organic material to form pyrite
68 crystals replicating in fine detail the anatomy of soft parts that can be otherwise lost (Raiswell
69 et al., 1993; Gabbott et al., 2004; Saleh et al., 2020b). Biogenic iron, from the decaying tissue,
70 is one possible source, initiating the mineralization process by forming pyrite nuclei (Saleh et
71 al., 2020c). However, abiotic Fe from sediments remains the main source for pyrite growth
72 (Saleh et al., 2020c). Although abiotic Fe was pivotal for soft-tissue preservation under oxic
73 and BSR conditions in the Fezouata Shale, the origin of this element remains speculative
74 (Gaines et al., 2012; Saleh et al., 2019). This study investigates the concentrations of trace and
75 rare earth elements in the Fezouata Shale aiming to answer the following questions: are
76 elemental sources (including Fe) authigenic or detrital? What are these sources (e.g., eolian,
77 volcanic, continental weathering)? Answering these questions will help to decipher the natural
78 processes that dictated soft-part preservation in the Fezouata Shale.

80 MATERIAL AND METHODS

81 Geochemical protocol

82 Two ~6.5m cores from the Fezouata Shale (check Appendix 1 information for stratigraphic
83 positions) were cut and scanned for their elemental composition using an Avaatech X-Ray
84 Fluorescence (XRF) Scanner at IFREMER laboratory, Plouzané, France. XRF data was
85 acquired with the precision of 1 analysis every 0.5cm and at 10kV. Considering that XRF data
86 is only semi-quantitative, the concentrations of Fe, Al, trace, and rare earth elements were
87 further explored using an HR-ICP-MS Element XR (Thermo Fisher Scientific) at the Pôle-
88 Spectrométrie-Océan (PSO, IUEM/Ifremer, Brest, France). 154 samples were taken from the
89 cores, one every 5 to 10cm. Then, powders were analyzed following a similar protocol to
90 Wilmeth et al. (2020). An expanded version of this protocol is presented in Appendix 1.

92 Data visualization and analyses

93 In order to determine if a correlation exists between Fe and Al their XRF data were plotted.
94 The degree of correlation between Fe and Al was confirmed by plotting ICP-MS data for
95 these elements and the Fe/Al ratio was calculated. In order to see if this value is impacted by
96 modern weathering, Fe and Al results were separated into two sets according to the degree of
97 modern weathering the samples encountered (see Appendix 1 for information on how modern
98 weathering was constrained). The newly obtained data were box-plotted and new Fe/Al ratios
99 were obtained. Fe and Al concentrations were also represented as box plots for levels with
100 and without exceptional fossil preservation. To further constrain modern weathering, the
101 concentrations of all measured elements from the two separate sample sets were plotted and
102 compared. Co/Th and La/Sc values were calculated and compared to data from McLennan et
103 al. (1983) (original diagram in Appendix 1) in order to test if there is a detrital, volcanic
104 source for Fe. A volcanic source was further investigated by comparing the concentration of
105 Sc, V, Cr, Co, Ni, Rb, Zr, Nb, Cs, La, Hf, Ta, Pb, and Th between the Fezouata Shale and
106 sediments deposited near active island arcs (McLennan, 2001). Furthermore, other potential
107 sources for Fe, including modern rivers, and loess were investigated following the same
108 comparative approach (McLennan, 2001). To quantify the dissimilarity between the Fezouata

109 Shale and these sources, a total dissimilarity index $TDiss_{index}$ was developed. This index can be
110 obtained by calculating the average of each elemental dissimilarity $EDiss_{index}$ between the
111 Fezouata Shale and the investigated sources according to the following equation (C is for
112 concentration, E is for element, and Ni is used as an example).
113

$$(E)diss_{index} = \left| 1 - \frac{C(E)_{investigated\ source}}{C(E)_{Fezouata\ Shale}} \right| ; \quad (Ni)diss_{index} = \left| 1 - \frac{C(Ni)_{investigated\ source}}{C(Ni)_{Fezouata\ Shale}} \right|$$

114
115 Note that this is a semi-quantitative index that is different from classical significance tests.
116 High index values mark a large heterogeneity between one source and the Fezouata Shale
117 without necessarily investigating if this difference is significant or not. The raw data are
118 provided in the Appendix 2.
119

120 RESULTS

121 XRF analyses show a relatively good correlation between Fe and Al ($R^2=0.6$, $N=2100$; Fig.
122 1A). This correlation is improved when using ICP-MS data ($R^2=0.68$, $N=154$; Fig. 1B). The
123 mean ratio of Fe/Al is equal to 0.32 ± 0.01 (Fig. 1B). This ratio did not change significantly
124 (t-test; $p=0.7064 > 0.05$) when separating non-modern weathered (Fe/Al= 0.34 ± 0.02 ,
125 $N=80$) from modern weathered sediments (Fe/Al= 0.32 ± 0.004 , $N=74$) (Fig. 2A). Both Fe
126 and Al are more enriched in levels with soft-part preservation (Fe= $6.6 \pm 0.27\%$, $N=29$; Al=
127 $21.45 \pm 1\%$; $N=29$) than in levels without exceptional preservation (Fe= $5.89 \pm 0.12\%$,
128 $N=125$; Al= $18.35 \pm 0.41\%$; $N=125$) (Fig. 2B). The difference between intervals with and
129 without exceptional fossil preservation (as indicated in Appendix 2) is significant for both Fe
130 (t-test; $p=0.0162 < 0.05$) and Al (t-test; $p=0.0023 < 0.05$).

131 In a similar way to iron, the concentrations of other elements (e.g., Cs, Sr, V) did not change
132 between weathered ($N=74$) and non-weathered sediments ($N=80$) except for some very minor
133 drifts in Zn and Pb concentrations (Fig. 3). The Co/Th ratio is generally less than 3, with a
134 mean of 1.07 ± 0.03 ($N=154$; Fig. 4), and the La/Sc ratio is generally between 1.2 and 3.6,
135 with a mean of 2.54 ± 0.03 ($N=154$; Fig. 4). Furthermore, the geochemical signature of the
136 Fezouata Shale is the most similar to modern rivers ($TDiss=0.31 \pm 0.06$) and less comparable
137 to the continental crust ($TDiss=0.49 \pm 0.06$), sediments deposited near active island arcs
138 ($TDiss=0.55 \pm 0.07$), and loess ($TDiss=0.71 \pm 0.04$) respectively (Fig. 5).
139

140 DISCUSSION

141 Al and Fe are well correlated in the Fezouata Shale (Fig. 1A, B). A similar correlation can
142 reflect (1) a detrital signal (Tribovillard et al., 2006), (2) an authigenic signal if the latter is
143 derived from a detrital source in what is effectively an isochemical system, or (3) an
144 authigenic signal in euxinic waters similar to the Black Sea (Dekov et al., 2020). In the
145 Fezouata Shale, the water column was dominantly oxic (Saleh et al., 2021b), favoring a
146 primary detrital source (either scenario 1 or 2). The non-intercepted correlation between Al
147 and Fe [in red; Fig. 1B ($y = 2.8709x + 1.621$)] is close to the intercepted trendline that passes
148 through the origin [in black; Fig. 1B ($y = 3.1255x$)], indicating that in the absence of Al, only
149 20% of Fe can be found. Moreover, Fe/Al is low (i.e., ~ 0.32), only 2/3 of the average shale
150 value of this ratio at ~ 0.5 (Lyons and Severmann, 2006). It is worth noting here that the low
151 ratio in the Fezouata Shale likely represents a local signal and does not necessarily reflect a
152 global value of Early Ordovician rocks. This ratio may reflect the original chemistry of the
153 basin, result from diagenesis, metamorphism, or even modern weathering, although the
154 Fezouata Shale was not affected by deep diagenesis and metamorphism (Saleh et al., 2020b,
155 c, 2021b). Moreover, both Fe and Al show no major difference between modern weathered
156 and non-recently weathered sediments in the Fezouata Shale (Fig. 2A) with non-significantly
157 different Fe/Al values. The minimal impact of modern weathering on Al and Fe
158 concentrations is also evidenced for other elements (Fig. 3). These findings align with the
159 results of previous studies showing that the main difference between non-modern weathered
160 and modern weathered sediments in the Fezouata Shale is limited to the leaching of Ca, S,
161 and C from altered sediments (Appendix 1; Saleh et al., 2020b, 2021b). In the absence of
162 metamorphism, pronounced diagenesis, and modern weathering, it is most likely that the low
163

164 Fe/Al reflects the original signal in the basin. The significant enrichment of Fe in levels with
165 exceptional preservation when compared to levels with no exceptional preservation (Fig. 2B),
166 and the correlation of this enrichment with significantly higher Al values (Fig. 2B) indicate
167 that detrital Fe was fluctuating in the Fezouata shale. This validates the findings of previous
168 studies showing that the probability of exceptional fossil preservation to occur in the Fezouata
169 Shale was augmented in specific levels in which Fe was present in the matrix (e.g., Saleh et
170 al., 2019).

171 Co/Th and La/Sc plots indicate that the previously suggested volcanic origin for detrital Fe in
172 the Fezouata Shale (Gaines, et al., 2012) is a minor source of chemical elements possibly
173 accounting for 20% of Fe in the formation (Fig. 4). For instance, detrital Co/Th is
174 considerably higher in sediments near volcanoes (i.e., Co/Th ~ 30; McLennan et al., 1983)
175 than it is in the Fezouata Shale (i.e., Co/Th <3 except one point; Fig. 4). Furthermore, an
176 aeolian source for Fe can be rejected because numerous elements show that the Fezouata
177 Shale is most comparable to rivers, followed by the average surface continental crust (Fig. 5).
178 The Fezouata Shale is almost twice more similar to rivers (smallest T_{diss} index) than to
179 siliciclastic sediments deposited near active island arcs (T_{diss}^{arcs} is slightly less than double
180 T_{diss}^{rivers}), and is least similar to aeolian sediments (T_{diss}^{loess} is higher than double T_{diss}^{rivers}). All
181 previous findings highlight that the source for Fe in the Fezouata Shale, is detrital, limited and
182 fluctuating, and resulting from surface continental weathering through precipitations, and
183 river inputs to the sea.

184 The positive impact of continental weathering on soft-tissue preservation may not have been
185 limited to the Ordovician. It has been recently documented that kaolinite correlates with
186 Cambrian and Precambrian soft-tissue preservation (Anderson et al., 2020, 2021). Kaolinite
187 damages bacterial membranes and slows down oxic decay (in a similar way to Fe, and Fe-rich
188 clay minerals; McMahan et al., 2016), and can even replicate labile anatomies in minute
189 details (Anderson et al., 2021). Moreover, it has been argued that the importance of kaolinite
190 in preserving soft-anatomies in the Cambrian can be further highlighted by the correlation of
191 this type of preservation with tropical settings, where kaolinite is typically formed (Anderson
192 et al., 2018; 2021). Kaolinite transport from the continents, where it is formed, to the sea must
193 have occurred through continental weathering. Kaolinite is not evidenced in the Fezouata
194 Shale and the primary clay precursor that aided the formation of Fe-rich clay minerals in this
195 formation is yet to be identified (Saleh et al., 2019). The lack of kaolinite can be attributed to
196 the deposition of the Fezouata Shale in polar settings. Regardless of the absence of kaolinite
197 in the Fezouata Shale, and its presence in many other sites with soft-tissue preservation (e.g.,
198 Anderson et al., 2020, 2021) it appears that continental weathering is a unifying process that
199 aided soft-part preservation through either Fe or kaolinite fluxes to the sea. In this sense, the
200 Cambrian–Ordovician world with elevated atmospheric CO₂ (Trotter et al., 2008) and intense
201 continental weathering might have favored soft-tissue preservation, which explains the
202 dominance of exceptional preservation during that time frame. A corollary of this finding is
203 that it is now possible to develop predictive approaches for the discovery of exceptionally
204 preserved fossils in Early Paleozoic rocks based on geochemical proxies quantifying the
205 magnitude of continental weathering.

206

207 **ACKNOWLEDGMENTS**

208 This paper is supported by grant no. 2020M683388 from the Chinese Postdoctoral Science
209 Foundation awarded to FS. This paper is a contribution to the TelluS-INTERRVIE project
210 ‘Géochimie d’un Lagerstätte de l’Ordovicien inférieur du Maroc’ (2019) funded by the INSU,
211 CNRS. We thank Bleuenn Guéguen for technical assistance during HR-ICP-MS analyses.
212 This paper is a contribution to the IGCP Projects 653 and 735. Three anonymous reviewers
213 are also thanked for their constructive remarks.

214

215 **REFERENCES**

- 216 Amonette, J.E., Russell, C.K., Carosino, K.A., Robinson, N.L., and Ho, J.T., 2003, Toxicity
217 of Al to *Desulfovibrio desulfuricans*: Applied and Environmental Microbiology, v. 69,
218 p. 4057–4066, doi:10.1128/AEM.69.7.4057-4066.2003
219 Anderson, R.P., Tosca, N.J., Gaines, R.R., Mongiardino Koch, N., Briggs, D.E.G., 2018, A
220 mineralogical signature for Burgess Shale–type fossilization: Geology, v. 46, p. 347–
221 350.

- 222 Anderson, R.P., Tosca, N.J., Saupe, E.E., Wade, J., Briggs, D.E.G., 2021, Early formation and
223 taphonomic significance of kaolinite associated with Burgess Shale fossils: *Geology*,
224 v. 49(4), p.355-359.
- 225 Anderson, R.P., Tosca, N.J., Cinque, G., Frogley, M.D., Lekkas, I., Akey, A., Hughes, G.M.,
226 Bergmann, K.D., Knoll, A.H., Briggs, D.E., 2020, Aluminosilicate haloes preserve
227 complex life approximately 800 million years ago. *Interface focus*, v. 10(4), p.
228 20200011.
- 229 Butterfield, N.J., 1990, Organic preservation of non-mineralizing organisms and the
230 taphonomy of the Burgess Shale: *Paleobiology*, v. 16, p. 272–286,
231 doi:10.1017/S0094837300009994.
- 232 Butterfield, N.J., 1995, Secular distribution of Burgess-Shale-type preservation: *Lethaia*, v.
233 28, p. 1–13, doi:10.1111/j.1502-3931.1995.tb01587.x.
- 234 Dekov, V.M., Darakchieva, V.Y., Billström, K., Garbe-Schönberg, C.D., Kamenov, G.D.,
235 Gallinari, M., Dimitrov, L., Ragueneau, O., Kooijman, E., 2020, Element enrichment
236 and provenance of the detrital component in Holocene sediments from the western
237 Black Sea: *Oceanologia*, v. 62(2), p.139-163.
- 238 Fu, D., Tong, G., Dai, T., Liu, W., Yang, Y., Zhang, Y., Cui, L., Li, L., Yun, H., Wu, Y., Sun,
239 A., 2019, The Qingjiang biota: a Burgess Shale-type fossil Lagerstätte from the early
240 Cambrian of South China: *Science*, v. 363 (6433), p. 1338–1342.
- 241 Gabbott, S.E., Xian-guang, H., Norry, M.J., Siveter, D.J., 2004, Preservation of Early
242 Cambrian animals of the Chengjiang Biota: *Geology*, 32, v. 901. [https://doi.org/
243 10.1130/G20640.1](https://doi.org/10.1130/G20640.1).
- 244 Gaines, R.R., Briggs, D.E.G., Orr, P.J., Van Roy, P., 2012, Preservation of giant
245 anomalocaridids in silica-chlorite concretions from the Early Ordovician of Morocco:
246 *Palaios*, v. 27, p. 317–325.
- 247 Guida, L., Saidi, Z., Hughes, M.N., and Poole, R.K., 1991, Aluminium toxicity and binding to
248 *Escherichia coli*: *Archives of Microbiology*, v. 156, p. 507–512,
249 doi:10.1007/BF00245400.
- 250 Hou, X., Siveter, David J., Siveter, Derek J., Aldridge, R.J., Cong, P., Gabbott, S.E., Ma, X.,
251 Purnell, M.A., Williams, M., 2004. *The Cambrian Fossils of Chengjiang, China: The
252 Flowering of Early Animal Life*. Blackwell.
- 253 Imlay, J.A., Chin, S.M., and Linn, S., 1988, Toxic DNA damage by hydrogen peroxide
254 through the Fenton reaction in vivo and in vitro: *Science*, v. 240, p. 640–642,
255 doi:10.1126/science.2834821.
- 256 Kapoor, K., and Arora, L., 1998, Aluminium induced toxicity and growth responses of
257 cyanobacteria: *Pollution Research*, v. 17, p. 25–31.
- 258 Lyons, T. W., Severmann, S. 2006, A critical look at iron paleoredox proxies: New insights
259 from modern euxinic marine basins: *Geochimica et Cosmochimica Acta*, v. 70(23), p.
260 5698–5722.
- 261 Martin, E.L.O., Pittet, B., Gutiérrez-Marco, J.-C., Vannier, J., El Hariri, K., Lerosey- Aubril,
262 R., Masrour, M., Nowak, H., Servais, T., Vandenbroucke, T.R.A., Van Roy, P.,
263 Vaucher, R., Lefebvre, B., 2016, The Lower Ordovician Fezouata Konservat-
264 Lagerstätte from Morocco: age, environment and evolutionary perspectives:
265 *Gondwana Res.*, v. 34, p. 274–283.
- 266 McLennan, S. M., Taylor, S. R., Eriksson, K. A. (1983). Geochemistry of Archean shales
267 from the Pilbara Supergroup, Western Australia: *Geochimica et Cosmochimica Acta*,
268 v. 47(7), p. 1211–1222.
- 269 McLennan, S.M., 2001, Relationships between the trace element composition of sedimentary
270 rocks and upper continental crust: *Geochemistry, Geophysics, Geosystems*, v. 2(4), p.
271 1-24.
- 272 McMahan, S., Anderson, R.P., Saupe, E.E., Briggs, D.E.G., 2016, Experimental evidence that
273 clay inhibits bacterial decomposers: implications for preservation of organic fossils:
274 *Geology*, v. 44, p. 867–870.
- 275 Nanglu, K., Caron, J.B., Gaines, R., 2020, The Burgess Shale paleocommunity with new
276 insights from Marble Canyon, British Columbia: *Paleobiology*, v. 46, p. 58–81.
- 277 Petrovich, R., 2001, Mechanisms of fossilization of the soft-bodied and lightly armored
278 faunas of the Burgess Shale and of some other classical localities: *American Journal
279 of Science*, v. 301, p. 683–726.

- 280 Raiswell, R., Whaler, K., Dean, S., Coleman, M., Briggs, D.E., 1993, A simple three-
 281 dimensional model of diffusion-with-precipitation applied to localized pyrite
 282 formation in framboids, fossils and detrital iron minerals: *Mar. Geol.*, v. 113, p. 89–
 283 100.
- 284 Saleh, F., Pittet, B., Perrillat, J., Lefebvre, B., 2019, Orbital control on exceptional fossil
 285 preservation: *Geology*, v. 47, p.103-106.
- 286 Saleh, F., Antcliffe, J.B., Lefebvre, B., Pittet, B., Laibl, L., Perez Peris, F., Lustri, L., Gueriau,
 287 P., Daley, A.C., 2020a, Taphonomic bias in exceptionally preserved biotas: *Earth
 288 Planet. Sci. Lett.*, v. 529, p.115873.
- 289 Saleh, F., Pittet, B., Sansjofre, P., Gueriau, P., Lalonde, S., Perrillat, J.-P., Vidal, M., Lucas,
 290 V., El Hariri, K., Kouraiss, K., Lefebvre, B., 2020b, Taphonomic pathway of
 291 exceptionally preserved fossils in the Lower Ordovician of Morocco: *Geobios*, v. 60,
 292 p. 99-115.
- 293 Saleh, F., Daley, A.C., Lefebvre, B., Pittet, B., Perrillat, J.P., 2020c, Biogenic iron preserves
 294 structures during fossilization: a hypothesis: Iron from decaying tissues may stabilize
 295 their morphology in the fossil record: *BioEssays*, v. 42, p.1900243.
- 296 Saleh, F., Bath-Enright, O.G., Daley, A.C., Lefebvre, B., Pittet, B., Vite, A., Ma, X.,
 297 Mángano, M.G., Buatois, L.A., Antcliffe, J.B., 2021a, A novel tool to untangle the
 298 ecology and fossil preservation knot in exceptionally preserved biotas. *Earth and
 299 Planetary Science Letters*, 569, p.117061.
- 300 Saleh, F., Vaucher, R., Antcliffe, J.B., Daley, A.C., El Hariri, K., Kouraiss, K., Lefebvre, B.,
 301 Martin, E.L., Perrillat, J.P., Sansjofre, P. and Vidal, M., 2021b, Insights into soft-part
 302 preservation from the Early Ordovician Fezouata Biota: *Earth-Science Reviews*, v.
 303 213, p.103464.
- 304 Tribouvillard, N., Algeo, T.J., Lyons, T., Riboulleau, A., 2006, Trace metals as paleoredox and
 305 paleoproductivity proxies: an update: *Chemical geology*, v. 232(1-2), p. 12-32.
- 306 Trotter, J.A., Williams, I.S., Barnes, C.R., Lécuyer, C., Nicoll, R.S., 2008, Did cooling oceans
 307 trigger Ordovician biodiversification? Evidence from conodont thermometry. *Science*,
 308 v. 321(5888), p.550-554.
- 309 Van Roy, P., Orr, P.J., Botting, J.P., Muir, L.A., Vinther, J., Lefebvre, B., El Hariri, K.,
 310 Briggs, D.E.G., 2010, Ordovician faunas of Burgess Shale type: *Nature*, v. 465, p.
 311 215–218., doi: 10.1038/nature09038.
- 312 Van Roy, P., Briggs, D.E., Gaines, R.R., 2015, The Fezouata fossils of Morocco; an
 313 extraordinary record of marine life in the Early Ordovician: *J. Geol. Soc.*, v. 172 (5),
 314 p. 541–549.
- 315 Wilmeth, D.T., Nabhan, S., Myers, K.D., Slagter, S., Lalonde, S.V., Sansjofre, P., Homann,
 316 M., Konhauser, K.O., Munoz-Saez, C., Van Zuilen, M.A., 2020., 2020, Depositional
 317 evolution of an extinct sinter mound from source to outflow, El Tatio, Chile:
 318 *Sedimentary Geology*, v. 406, p.105726.
- 319 Wilson, L.A., Butterfield, N.J., 2014, Sediment effects on the preservation of Burgess Shale–
 320 type compression fossils: *Palaios*, v. 29, p. 145–154, doi:10.2110/palo.2013.075.

321 322 **FIGURE CAPTIONS**

323
324 **Figure 1.** (A) XRF Al-Fe correlation in the Fezouata Shale (blue dots, and red trendline).
 325 (B) ICP-MS Al-Fe correlation (blue dots, and red trendline). The black lines in (A) and (B)
 326 represent intercepted trends for this correlation passing through the origin (0 value).

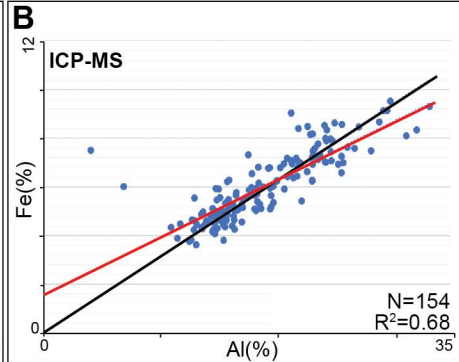
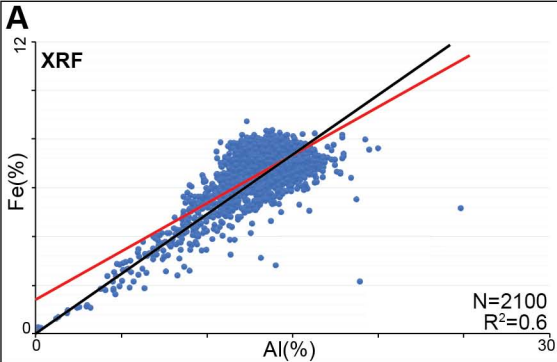
327
328 **Figure 2.** (A) Fe and Al differences between modernly weathered and non-modernly
 329 weathered sediments. (B) Fe and Al differences between levels with and without
 330 exceptionally preserved fossils.

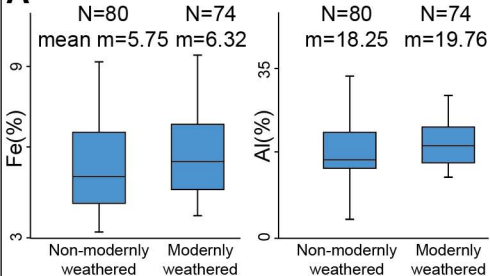
331
332 **Figure 3.** Trace and rare earth elements differences between modernly weathered and non-
 333 modernly weathered facies.

334
335 **Figure 4.** Co/Th and La/Sc ratios in the Fezouata Shale plotted on the McLennan et al.
 336 (1983) diagram.

337

338 **Figure 5.** Chemical signature for the Fezouata Shale plotted against elemental data from
339 modern rivers, average surface continental crust, loess, and siliciclastic sediments near active
340 island arcs.



A**B**